Supporting Information for

Substituent-Directed Assembly of 1D and 2D Silver Aryl Tellurolates with Tunable Emission

Komal Rani,[a,b] Anietie W. Williams,[b] Tarun Kaushik,[a,b] Daniel W. Paley,[c] Maggie C. Willson,[a,b] Masha Aleksich,[a,b] Patience A. Kotei,[a,b] Mark R. Warren,[d] Adrian P. Mancuso,[d,e] Kerry Gilmore,[b] Aaron S. Brewster,*[c] J. Nathan Hohman*[a,b]

Author Affiliations:

[a]Institute of Materials Science, University of Connecticut, CT, 06269, USA

[b]Department of Chemistry, University of Connecticut, CT, 06269, USA

[c]Molecular Biophysics and Integrated Bioimaging Division, Lawrence Berkeley National Laboratory, Berkeley, CA, 94720, USA

[d]Diamond Light Source, Harwell Science & Innovation Campus, Oxfordshire OX11 0DE, U.K.

[e]La Trobe University, Melbourne, Australia, VIC 3086

Table of Contents.

Experimental

Reduction synthesis pathway

A sample of AgTe-3M was synthesized using a redox pathway. In a two-neck round-bottom flask equipped with a Schlenk line on one neck and a septum on the other, bis(3-methoxyphenyl) ditelluride (101 mg, 0.22 mmol) was dissolved in ethanol (10 mL). To this solution, sodium borohydride ($NaBH_4$, 0.42 g, 2.0 equiv.) was added, and the reaction mixture was stirred for 30 minutes, generating the corresponding sodium tellurolate species. Then, silver nitrate ($AgNO_3$, 36 mg, 0.25 equiv.) was dissolved in ethylamine (10 mL) and added to the flask, and the reaction was allowed to sit at 150 rpm stirring for 24 hours. The product was isolated and purified as AgTe-4M and AgTe-3M samples synthesized using Ag as the metal source in this study. These findings establish that metal-organic tellurolates can be synthesized using either tellurolate reagents or ditelluride precursors. Both synthetic pathways yielded the same product; consequently, the more straightforward one-pot procedure utilizing bis(3-methoxyphenyl) ditelluride and other ditellurides were adopted for the preparation of subsequent samples.

Characterization

The obtained powder products were directly used for further characterization by SEM, pXRD, UV-Vis, Fluorescence, TGA.

Scanning Electron Microscopy and Energy Dispersive X-ray Spectroscopy

For the collection of scanning electron microscopy (SEM) and Energy Dispersive X-ray Spectroscopy (EDX) data, a powder sample was added in methanol (1 mg/mL) and sonicated for 5 minutes to separate the crystals and form a suspension. A 5x7 mm precut silicon wafer chip was cleaned using compressed nitrogen gas for several seconds, after which it was placed on a clean, flat surface. Two drops of the sonicated suspension were applied to the wafer and allowed to dry, enabling the evaporation of the solvent. Subsequently, the wafer was mounted on a standard SEM pin stub using double-coated carbon conductive tabs. The stub was then dried with nitrogen gas to remove any loose crystals or debris. Finally, the sample was imaged using a FEI Nova NanoSEM 450.

UV-Vis

For collecting absorption data, a Cary 4000 UV-Vis spectrometer (Agilent; Santa Clara, CA) was used. Solid powdered sample was crushed carefully and placed in the center of Internal DRA powder cell holder and absorption data was collected.

Fluorescence

For collecting fluorescence data, a Cary Eclipse Fluorescence Spectrometer (Agilent; Santa Clara, CA) was used. 3 mg of sample was added into 3 mL of methanol and sonicated for 2 minutes to form suspension. Solution was transferred into fluorescence quartz cuvettes for data collection. Tethrene and AgTe-4M were excited at 400nm and AgTe-3M at 500nm.

Powder X-Ray Diffraction

For collecting pXRD data, a Bruker D2 Phaser owned by COR^2E at the University of Connecticut was used. Dried powder sample was crushed and filled in the cavity of a zero diffraction Si plate. The surface of powder was smoothed out to the level of plate with a clean glass microscope slide before loading. XRD pattern was collected from 2-60 two theta degrees.

NMR

To confirm the successful synthesis, Nuclear Magnetic Spectroscopy was performed for bis(3-methoxyphenyl) ditelluride and bis(4-methoxyphenyl) ditelluride. The crude product was purified by column chromatography using hexanes to afford the target compound, bis(3-methoxyphenol) ditelluride as a red oil (0.87 g, 74% yield): ^{1}H NMR (400 MHz, $CDCl_3$): δ ppm: 7.41-7.34 (m, 4H), 7.08 (t, J = 15.8 Hz, 2H), 6.80-6.74 (m, 2H), 3.78 (s, 6H). For obtaining bis(4-methoxyphenyl) ditelluride, same purification method was done using hexanes to afford orange yellow oil (0.95 g, 81% yield): ^{1}H NMR (400 MHz, $CDCl_3$): δ ppm: 7.72 (d, J = 8.8 Hz, 4H), 6.77 (d, J = 8.7 Hz, 4H), 3.83 (s, 6H). This data (Figure S2) matches with reported data.[1,2]

TGA

For collecting thermogravimetric analysis data, a TGA-Q500 Thermobalance from TA instruments was used. Solid powder sample approximately 10 mg was taken on a clean platinum pan and loaded onto the instrument. Data was recorded from 25°C to 800°C under nitrogen gas flow.

Crystallography

Crystallography measurements were carried-out at the I19-EH2 beamline at Diamond Light Source using a wavelength of 0.48590 Å and a four-circle Newport diffractometer with XYZ SLC-2430 linear piezo sample stages equipped with a Dectris Eiger CdTe X 4M detector. A suspension

of AgTe-4M in formalin oil (Fobblin Y 3300 Sigma Aldrich) was pulled through a 400-well silicon nitride grid using a light vacuum and mounted on the diffractometer.

The AgTe-4M structure was solved using SHELXT[3] and refined via SHELXL[4] in Olex2[5]. A RIGU rigid-bond restraint was applied to the carbon and oxygen atoms. The aryl ring was modeled as a rigid hexagon and a planarity restraint was applied to the Te-aryl-O fragment. The aromatic hydrogen atoms were refined with riding coordinates and the methyl hydrogens were refined as an idealized rotating methyl group. One reflection (0 0 2) was partially covered by the beamstop and was omitted from refinement. We were unsuccessful in solving the AgTe-3M. There are several possibilities for this, especially sample phase impurity. In a recent, second beamtime attempt we crystallographically identified a telluric methyl ester byproduct. We postulate that under these conditions the further oxidation of the precursor is a source of interference.

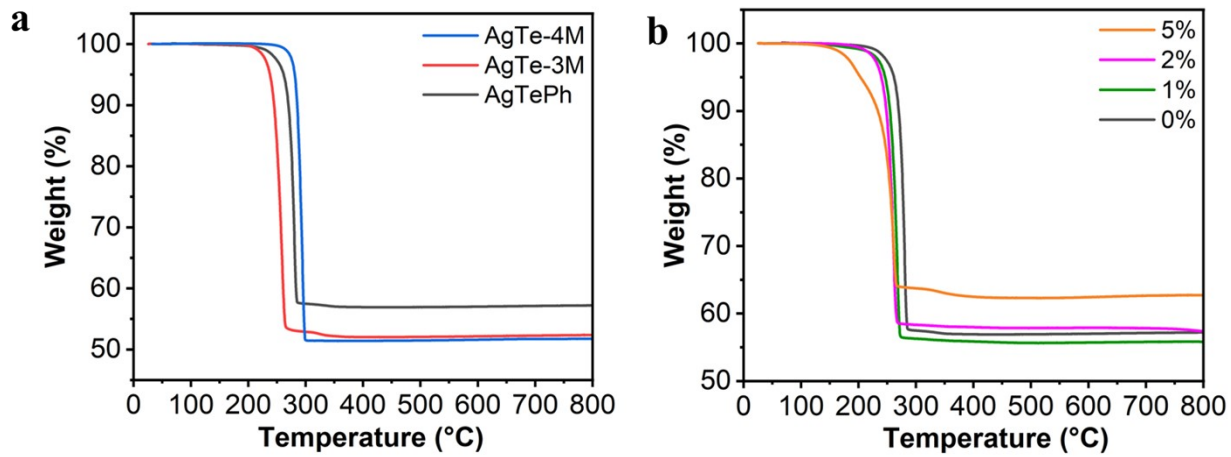

Figure S1. a) Thermogravimetric analysis for decomposition temperature of AgTePh, AgTe-3M and AgTe-4M b) Thermogravimetric analysis of 0%, 1%, 2% and 5%.

TGA for contaminated samples was conducted for quantitative purposes (**Figure S1**), the mass loss data was used to calculate the percentage yield of the product by interpreting the thermal behavior of each component in the contaminated sample.

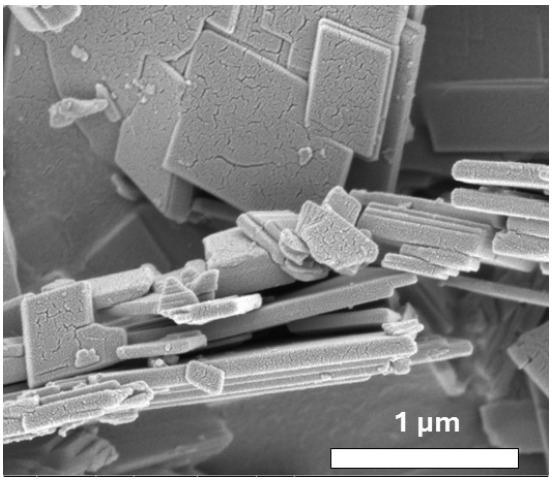

Figure S2. SEM showing cross-sectional view of the crystals AgTe-4M.

Figure S2 shows the cross-sectional view of crystals AgTe-4M revealing the approximate thickness of the typical crystals is around 100nm, corresponding to between 55 to 56 layers at 1.8nm per layer thickness.

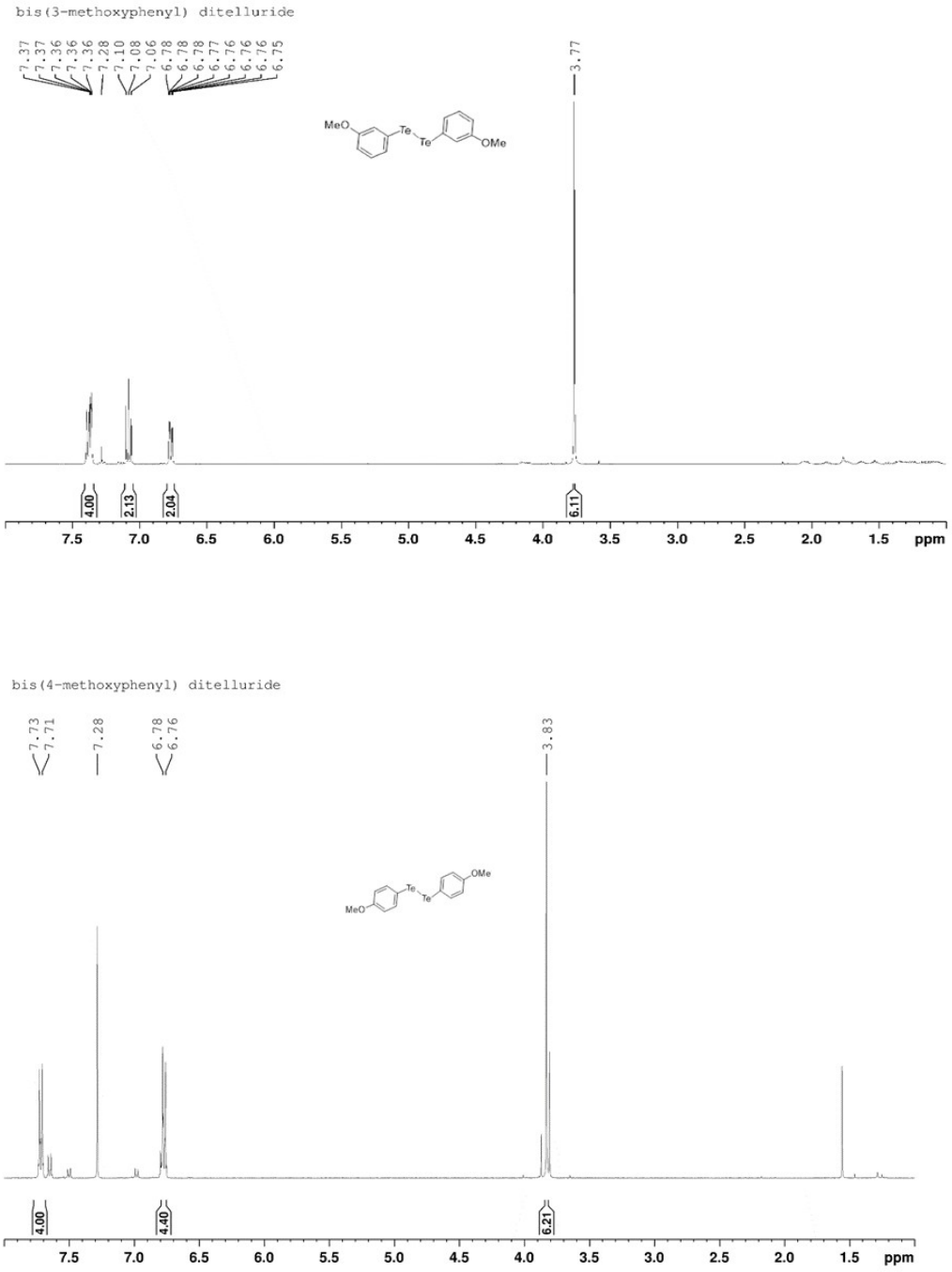

Figure S3. NMR data for bis(3-methoxyphenyl) ditelluride (top) and bis(4-methoxyphenyl) ditelluride (bottom).

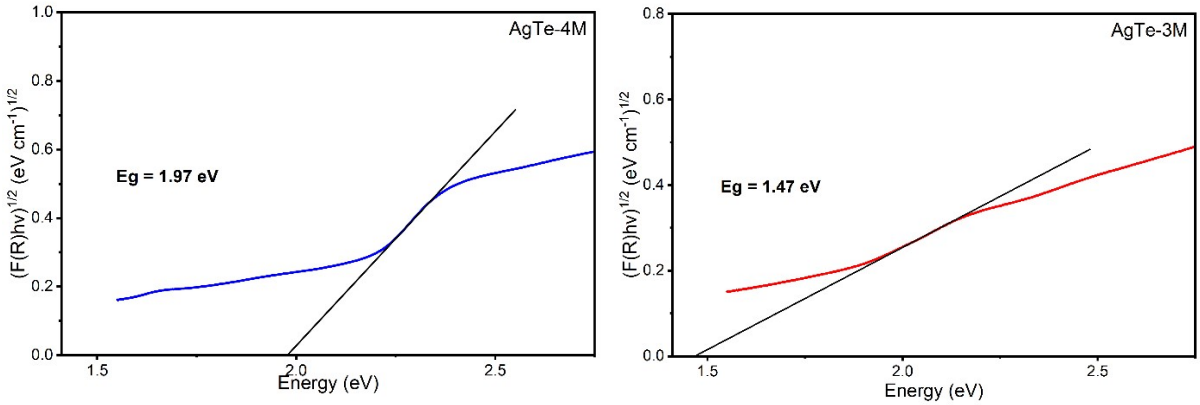

Figure S4. Tauc Plot for optical band gap estimation of AgTe-4M and AgTe-3M

For powdered samples, diffuse reflectrance (%) was obtained using the UV-Vis spectrometer. Reflectance values were converted to absolute reflectance and transformed using the Kubelka-Munk function. Tauc plots of $(F(R)hv)^{1/2}$ were used to estimate optical band-gap using linear region extrapolation on energy axis. These estimated values are consistent with the orange and red emission frequency of the two derivatives.

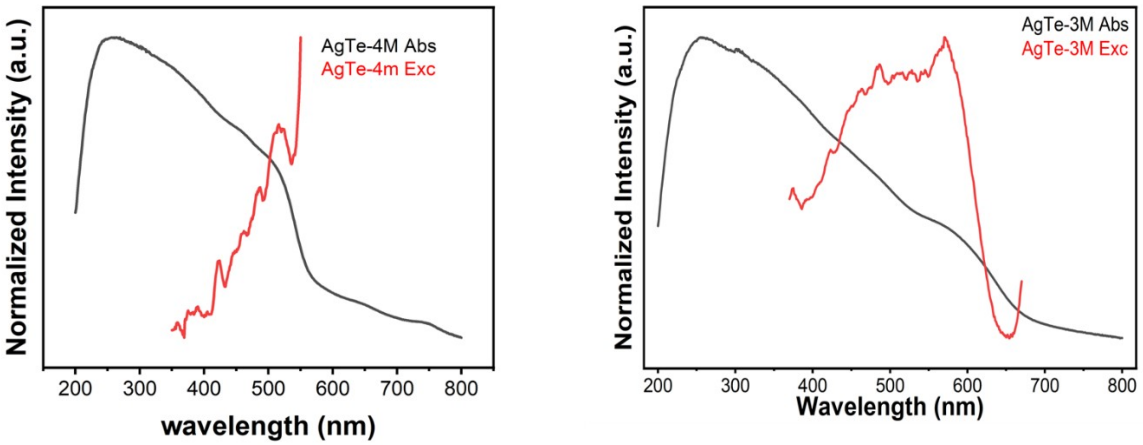

Figure S5. Comparison of absorption spectra and excitation spectra of AgTe-4M (left)and AgTe-3M (right)

The excitation spectra for both the powders were recorded near the emission maxima of AgTe-4M (584nm) and AgTe-3M (700nm). Previous studies on AgTePh (tethrene) suggest self-trapping of free excitons via local lattice deformations accompanied by broadened excitonic transitions and strong exciton-phonon coupling.[6] AgTePh exhibits a selective excitation profile where efficient broadband STE (self-trapping excitons) emission is generated primarily from above-gap excitonic absorption, while sub-gap absorption produces much weaker, spectrally-distinct emission. Previous studies have discussed the mismatch in lifetimes for selenium-based MOCha, mithrene, and tellurium-based MOCha, tethrene.[6,7] AgTe-3M and AgTe-4M display mismatches between their excitation and absorption spectra, indicating self-trapped excitons or strongly relaxed emissive states rather than simple band-edge recombination. The STE nature of these mismatches requires further experimental and computational investigation and is reserved for future studies.

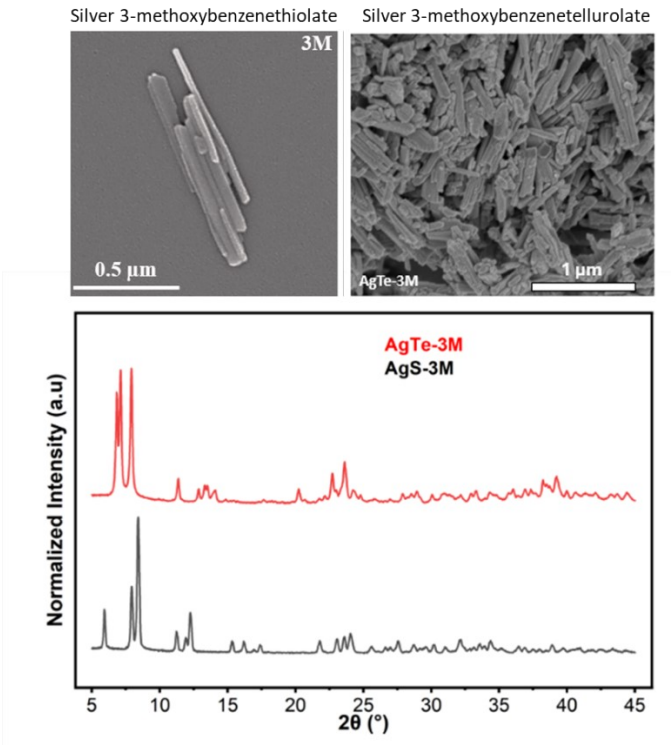

Figure S6. SEM images and pXRD of Silver 3-methoxybenzenethiolate and Silver 3-methoxybenzenetellurolate (AgTe-3M)

Recent studies report on the structures of Silver 3-methoxybenzenethiolate (AgS-3M) and Silver 4-methoxybenzenethiolate (AgS-4M).[8] Notably, AgS-4M (orthorhombic, a=7.273 Å, b=17.165 Å, c=5.918 Å) and AgTe-4M (orthorhombic, a=7.4688 Å, b=5.943 Å, c=35.972 Å) exhibit closely matched lattice parameters, with two axes nearly identical and third approximately doubled in the tellurolate, alongside similar pXRD patterns and 2D layered morphologies observed by SEM. These analogies suggest that AgTe-3M likely adopts a structure analogous to AgS-3M, as indicated by the comparable pXRD and SEM in **Figure S**7.

a

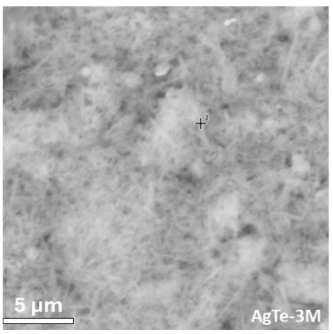

Element Number	Element Symbol	Element Name	Atomic Conc.	Weight Conc.
6	C	Carbon	63.26	28.37
14	Si	Silicon	16.79	17.60
8	O	Oxygen	8.93	5.34
52	Te	Tellurium	5.88	28.00
47	Ag	Silver	5.14	20.70

b

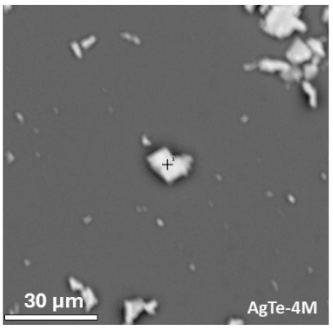

Element Number	Element Symbol	Element Name	Atomic Conc.	Weight Conc.
6	C	Carbon	60.14	27.80
14	Si	Silicon	26.76	28.91
47	Ag	Silver	4.80	19.91
52	Te	Tellurium	4.25	20.89
8	O	Oxygen	4.05	2.49

Figure S7. SEM images and pXRD of Silver 3-methoxybenzenethiolate and Silver 3-methoxybenzenetellurolate (AgTe-3M)

Energy-dispersive X-ray spectroscopy (EDX) analysis of AgTe-4M and AgTe-3M confirms the expected Ag:Te ratio of ~1:1 across multiple crystals, consistent with their stoichiometries. Silicon signals arise from the substrate. This data verifies the phase purity and compositional integrity of both MOChas.

REFERENCES

1 Y. Deng, X. Zeng, H. Xu, J. Liu, J. Zhang, D. Hu and J. Xie, *New Journal of Chemistry*, 2022, **46**, 20078–20081.

2 M. Akiba, V. Lakshmikantham, K.-Y. Jen and M. P. Cava, *Downloaded via UNIV OF CONNECTICUT on*, UTC, 1984, vol. 49.

3 G. M. Sheldrick, *Acta Crystallogr. A*, 2015, **71**, 3–8.

4 G. M. Sheldrick, *Acta Crystallogr. C Struct. Chem.*, 2015, **71**, 3–8.

5 O. V. Dolomanov, L. J. Bourhis, R. J. Gildea, J. A. K. Howard and H. Puschmann, *J. Appl. Crystallogr.*, 2009, **42**, 339–341.

6 W. S. Lee, Y. Cho, E. R. Powers, W. Paritmongkol, T. Sakurada, H. J. Kulik and W. A. Tisdale, *ACS Nano*, 2022, **16**, 20318–20328.

7 K. Yao, M. S. Collins, K. M. Nell, E. S. Barnard, N. J. Borys, T. Kuykendall, J. N. Hohman and P. J. Schuck, *ACS Nano*, 2021, **15**, 4085–4092.

8 M. Aleksich, Y. Cho, D. W. Paley, M. C. Willson, H. N. Nyiera, P. A. Kotei, V. Oklejas, D. W. Mittan-Moreau, E. A. Schriber, K. Christensen, I. Inoue, S. Owada, K. Tono, M. Sugahara, S. Inaba-Inoue, M. Vakili, C. J. Milne, F. DallAntonia, D. Khakhulin, F. Ardana-Lamas, F. Lima, J. Valerio, H. Han, T. Gallo, H. Yousef, O. Turkot, I. J. B. Macias, T. Kluyver, P. Schmidt, L. Gelisio, A. R. Round, Y. Jiang, D. Vinci, Y. Uemura, M. Kloos, A. P. Mancuso, M. Warren, N. K. Sauter, J. Zhao, T. Smidt, H. J. Kulik, S. Sharifzadeh, A. S. Brewster and J. N. Hohman, *Adv. Funct. Mater.*, DOI:10.1002/adfm.202414914.